China Steel Technical Report, No. 27, pp.50－56, (2014)

A Comprehensive Performance Evaluation on an Antiscalant for the Open-Loop Cooling Water System

HSIN-HUNG OU and JIEN-LEIN HAN

New Materials Research & Development Department
China Steel Corporation

An environmentally friendly antiscalant (ECO-T6) with half the phosphate levels of a Commercial Product (COMP) was developed to suppress calcite formation. The inhibition performance and mechanism of ECO-T6 were examined based on a comprehensive approach including chronoampermetric measurement, particle size distribution analysis, scanning electronic microscopy, X-ray diffraction spectrometry and light scattering spectroscopy. The results obtained from chronoampermetric measurement verified that ECO-T6 was as effective as the COMP in inhibiting $CaCO_3$ formation. Optical microscopy image and particle size distribution analysis indicated that the distortion of calcite crystal made by ECO-T6 was different from that by COMP. X-ray diffraction analysis further confirmed the successful transformation of rhombohedric calcite into the vaterite phase in the presence of antiscalant. Light scattering spectroscopy was particularly established to investigate the inhibition mechanism and kinetics of $CaCO_3$ formation with antiscalant. The kinetics of $CaCO_3$ formation appeared to be first order in the case of either control experiment or the COMP whereas $CaCO_3$ formed in the presence of ECO-T6 followed a zero-order reaction.

Keywords*: Antiscalant, Cooling water system, Phosphate*

1. INTRODUCTION

Cooling water quality and availability are critical for maintaining production at most operating facilities. In addition to issues related to corrosion and microorganism growth in the cooling water system, another important concern is the possible mineral deposition (scale formation), which is likely to be associated with make-up water quality and the surrounding environment around the cooling tower[1]. In fact, cooling water systems suffer great economic losses owing to the severe mineral deposition and adhesion onto the heat equipment surface, along with the problems of corrosion and biofouling. For example, the clogging of pipes is the consequence of the scale formation which reduces heat transfer efficiency, leading sometimes to the shutdown of an industrial plant in the worst cases. Increased energy and maintenance costs, as well as plant shutdown, are some of the economic penalties resulting from scale deposition. Scale is mainly constituted of calcium carbonate ($CaCO_3$), which has three major crystalline forms including calcite (rhombohedric structure), aragonite (orthorhombic) and vaterite (hexagonal)[2,3]. The nature and rate of scaling is dependent on the physical, chemical and bacteriological characteristics of cooling water.

Cooling water systems could be restored from scaling problems using either chemical or physical approaches. In general, the efficiency of physical treatment like magnetic/electronic conditioners and ultrasound equipment are far less effective than that of chemical treatment and the performance of a physical approach is still subject to debate as a reaction mechanism[4]. Specialty chemicals for water treatment have been in use for over a century. Not only is there a lot of commercial products available but the reaction mechanism is well understood. Commonly used antiscalants are chemical compounds derived from chelating agents. These chelating agents either form calcium or magnesium complexes and decrease the supersaturation level, or are able to weaken the adherence to surfaces by its morphological dissymmetry. The suggested inhibition mechanism of $CaCO_3$ formation is dependent on the physical and chemical features of the antiscalant[5]. For example, a copolymer with simultaneously carboxylic and sulfonic groups could chelate Ca^{2+} to form stabilized and dissoluble chelates. Some antiscalants are also able to modify the $CaCO_3$ crystal. The mechanism suggested for this inhibition is the adsorption of antiscalant on the calcite surface, which blocks the active crystal growth sites. In other words, the involvement of antiscalant is likely to delay germination, slow down crystal rate, favor homogeneous germination to the detriment of heterogeneous germination or deforming

the crystals, giving them a friable structure that weakens its adherence to a pipeline surface.

In addition to some common phosphate-based chemicals, some environment friendly antiscalants have been developed[6,7]. In this regard, polyaspartic acid, polyepoxysuccinic acid, poly-alkyl-epoxysuccinic acid and natural polymers are commonly seen, however, most of them are not only less efficient but expensive as compared to the commercial products, resulting in an impossible use in field. As far as the performance and economic costs are concerned, the phosphate-based chemicals or derivatives are still popular with no doubt. Since phosphate is likely to be regulated in the near future by The Environmental Protection Agency, a promising attempt that corresponds to the increasingly strict environmental regulations is to develop a formulation exhibiting a comparative performance with less phosphate content to break the tradeoff between economic costs and environmental policy. In this study, an antiscalant formulation with less phosphate and comparative price was developed. The inhibition performance of $CaCO_3$ formation with the developed antiscalant was also verified based on a comprehensive approach including chronoampermetric measurement, scanning electronic microscopy, X-ray diffraction spectrometry, particle size distribution analysis and light scattering spectroscopy.

2. EXPERIMENTAL METHOD

2.1 Evaluation of performance of antiscalant

The methods designed to evaluate the performance of the developed antiscalant include calcium ion measurement, chronoamperometry analysis and light scattering spectroscopy. Regarding the procedure of calcium ion measurement, 1000 ml of DI water and certain standard $CaCl_2$ solution containing 600 mg Ca^{2+} was firstly added into an appropriate flask, which was followed by an addition of 50 ppm antiscalant. $NaHCO_3$ standard solution containing 1200 mg of HCO_3^- was added into the above solution right after the addition of the antiscalant. The control experiment was also carried out with the absence of antiscalant in the same way as mentioned above. Ca^{2+} concentration in the test solution was quantified by 0.01 m EDTA solution and plotted versus time profile for the preliminary investigation. All the experiments were carried out at 35℃ in triplicate.

Chronoamperometry curves were obtained with a conventional three-electrode cell assembly by polarizing carbon steel electrodes to -0.9 V (v.s. SCE) at 35℃ in a test solution for 3 hours. The preparation procedure of the test solution was the same as that mentioned above. The cell consists of a Pt electrode and a $Ag/AgCl_2$ electrode as counter and reference electrodes, respectively. The material used for constructing the working electrode was carbon steel that had the following chemical composition (wt %): C, 0.24; Si, 0.41; Mn, 2.3; P, 0.04; S, 0.04; balance Fe. Prior to the measurement, the exposed area of 1 cm^2 was mechanically abraded with a series of emery papers of variable grades, starting with a coarse grade and proceeding in steps to the finest grade.

A state of the art technique in dynamic light scattering was exploited to monitor the $CaCO_3$ crystallization kinetics. A stability index known as the Turbiscan Stability Index (TSI) developed by The Formulaction Company was used to determine the variation of light intensity detected in the sample. Thanks to the TSI, determination of the crystallization kinetics of $CaCO_3$ appears to be possible, as the crystalline process might have an influential effect on the light behavior and intensity during the time of interest. The transmission light intensity in the absence and presence of antiscalants were recorded over time and converted into TSI values. The experiments were carried out in 40 ml glass tubes at 35℃ for 1 day.

2.2 Characterization of precipitated powder in the absence and presence of antiscalant

The precipitated $CaCO_3$ particles from the test solutions after aging overnight at 80℃ were retrieved for further analysis including X-Ray Diffraction (XRD) analysis, Particle Size Distribution (PSD) measurement, and Scanning Electronic Microscopy (SEM). Using the BRUKER D8 Advanced X-ray Diffraction instrument, a XRD was performed to identify the crystal phase with and without the involvement of antiscalant. XRD data was collected using Cu Kα radiation (30 kV, 20 mA) with a diffracted beam monochromator. Scans were taken over a range of 10 to 60°. Particle size istribution measurement was carried out with multisizer 3 using an electrical sensing zone method (Beckman Coulter). The FE-SEM and Energy Sispersive X-ray spectroscopy (EDX) were used to investigate morphology and chemical composition of the $CaCO_3$ samples.

3. RESULTS AND DISCUSSION

3.1 Inhibition performance of antiscalant

Calcium ion concentrations in the absence and presence of antiscalant over time are shown in Fig.1. As demonstrated, there is a rapid drop in the concentration of calcium ion in the control experiment, indicating $CaCO_3$ crystallization over time at the expense of calcium ions in the solution. Comparatively, the calcium ion concentration is relatively stable in the presence of antiscalant and starts to drop off after 100 minutes in the case of the Commercial Product (COMP) whereas no significant decrease in calcium ion concentration

was observed with ECO-T6. This result can be explained by the fact that the stability of calcium ion with ECO-T6 is better than that with the COMP, as ECO-T6 consists of gluconate, which is an effective chelating reagent to form stabilized and dissoluble chelates. This possible explanation is further verified by observing the transparency of solution in the presence of ECO-T6, being relatively clear as compared to that with the COMP. However, the authentic performance of scale inhibition by antiscalant is subject to a synergistic capability toward calcium ion dispersion and calcite crystal distortion, and so this result only reveals that ECO-T6 dominates over the COMP in calcium ion dispersion.

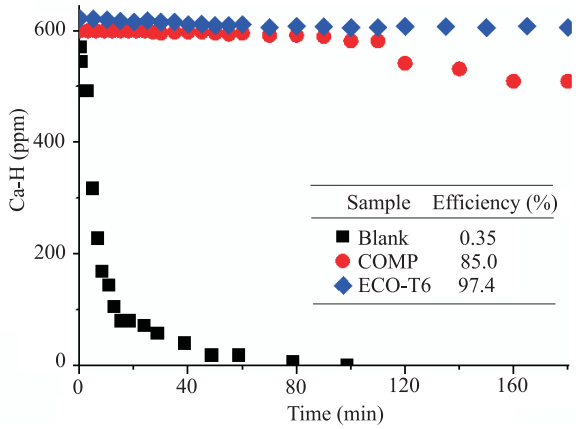

Fig.1. Ca^{2+} concentration profile over time in the absence and presence of antiscalants.

In addition to the concentration profile of calcium ions over time, chronoamperometry measurement has been reported to be a valid approach to evaluate the performance of antiscalant despite the scale generated in the electrochemical experiment is of a difference nature to that formed in the field. Figure 2 shows the chronoamperometry curves for polarized carbon steel electrodes in the test solutions in the absence and presence of antiscalant at 35℃. In the control experiment, the curve features two regions including $CaCO_3$ growth and increasing coverage of the electrode surface. The intersection point of the extrapolated lines from two separate regions signifies the scaling time at which total coverage of the electrode surface was attained. As shown, the time for total $CaCO_3$ coverage of the electrode surface is around 40 minutes in the control experiment. In the case of antiscalant being involved, the current remained relatively stable during the time of interest as compared to that of the control experiment. This result reveals that ECO-T6 performs as efficient as the COMP in inhibiting $CaCO_3$ formation. However, a gradual decrease in current in the case of ECO-T6 was observed whereas the current with the COMP steadily rises over time. The result obtained from the COMP appears to be implausible, as possible $CaCO_3$ deposition on the electrode surface appears not to take place. Two possible explanations are proposed in that $CaCO_3$ particles formed with the COMP are geometrically not accessible to the electrode surface and the other is that some chemicals of the COMP are responsible for corrosion inhibition but are thermodynamically unfavorable to adsorb over the electrode surface, leaving more channels for ion transportation (A protective film layer was clearly seen right above the steel surface in the case of ECO-T6 whereas there is no film observed with the COMP, images not shown).

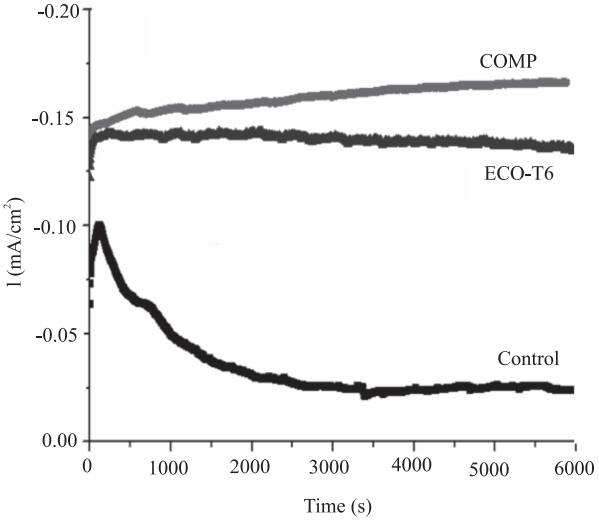

Fig.2. Chronoamperometric curves obtained on carbon steel electrode at 35℃ in the absence and presence of antiscalants.

3.2 Characterization of $CaCO_3$ powder in the absence and presence of antiscalant

3.2.1 SEM observation

SEM images of $CaCO_3$ precipitations in the presence and absence of antiscalant demonstrated the changes in both the size and shape of the precipitates due to antiscalant addition (Fig.3a). Rhombohedral structures along with trace amounts of rod-shaped particles are present in the control experiment, which is indicative of the calcite and aragonite polymorph, respectively[8]. Comparatively, a dramatic change in the particle morphology and uniformity was observed in case where antiscalant was involved. The rounding of the corners and pitting of $CaCO_3$ particle surfaces are characteristics of redissolution of crystals. In terms of the particle morphology with ECO-T6, the particles have more irregular shape and less regular rhombohedral structure (Fig.3b). In addition to having layered

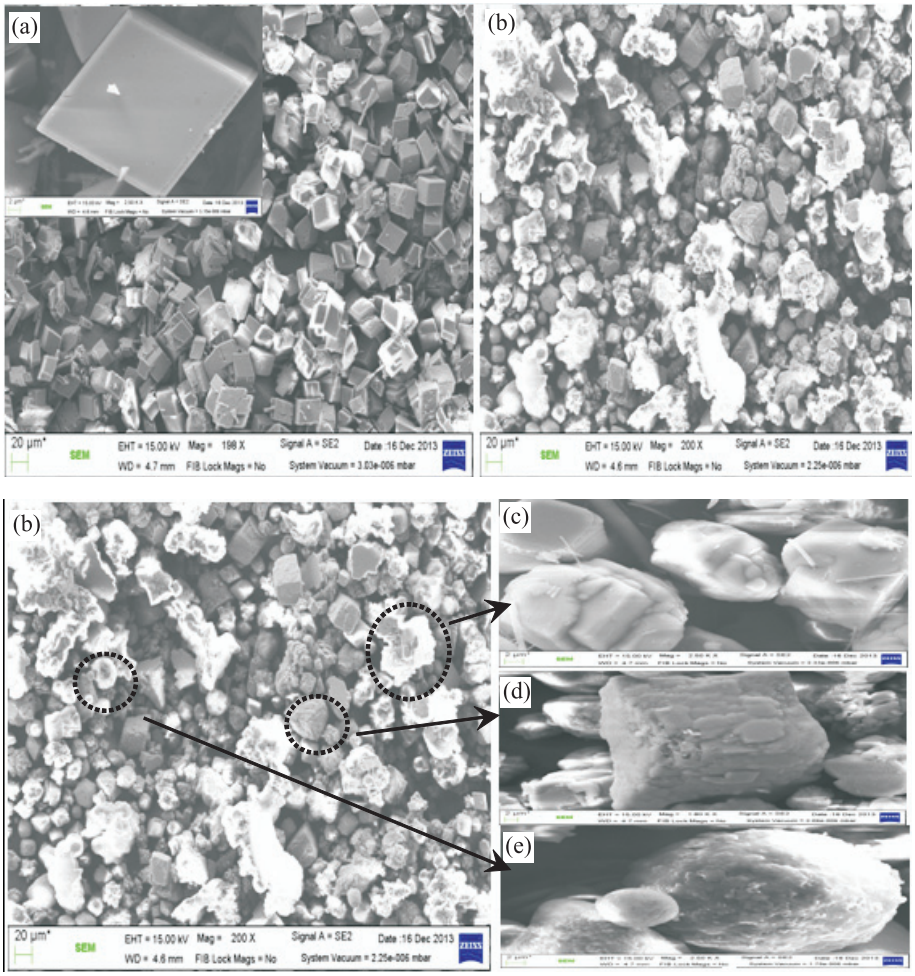

Fig.3. Structural morphologies of $CaCO_3$ in the absence (a) and presence (b,c,d,e) of ECO-T6.

structures (Fig.3c) and less well-defined edges in the rhombohedral calcite (Fig.3d), a spherical structure with rough edge morphology was also observed (Fig.3e). On the other hand, SEM images appear to demonstrate that ECO-T6 favored particle agglomeration which might be the reason for the formation of a layered structure. In comparison, $CaCO_3$ with the COMP presents most of the particle sizes smaller than 2 μm in addition to a trace amount of rhombohedral structures with rough edges (image not shown). Two distinguishable $CaCO_3$ morphologies were observed with the COMP and ECO-T6 which are likely to feature two different suppression mechanisms of $CaCO_3$ formation.

3.2.2 PSD analysis

The PSD pattern in the control experiment illustrated a symmetric bell-shaped curve (Gaussian distribution) with a mean diameter of 25.61 μm. However, the PSD pattern was transformed into a bimodal and skewed curve in the case of antiscalant being involved (Fig.4). As soon as the antiscalant present in the $CaCO_3$ crystallization process, the particle diameters represented by the curve below 2 μm are nucleated particles, while curves in the larger size range account for formed crystals[9]. The curve with ECO-T6 verified that the majority of particles formed were within the larger particle size range (30 to 60 μm), which was along with trace amounts of 2 μm particles. Comparatively, the particle size with the COMP is homogeneously distributed in the range of 2 to 20 μm in addition to another major portion of particle sizes larger than 20 μm. More dramatic reductions in particle size were observed for the addition of the COMP whereas the presence of ECO-T6 resulted in a significant increase in particle size. According to the PSD curves, ECO-T6 appears to be as effective as the COMP for distorting the calcite growth but with a different inhibition mechanism. This result corresponds to the SEM images (Fig.3) and illustrations from the chronoamperometry measurements

shown in Fig.2, whereas any particles of a relatively small geometrical diameter were hardly attracted towards the electrode surface in a moderate turbulent condition, resulting in a slight increase in current.

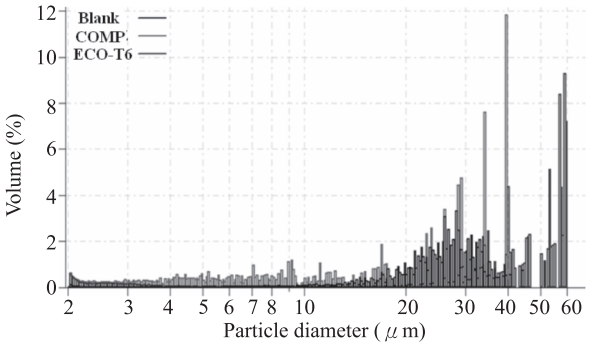

Fig.4. Particle size distribution patterns of $CaCO_3$ in the absence and presence of antiscalants.

The monodispersity D90/D10, which is defined from the size distribution curve at accumulative of 10% and 90%, was also calculated to assess the uniformity of the distribution of particle size. D90/D10 in the control experiment is 2.15 whereas the values for ECO-T6 and COMP are 11.58 and 12.55, respectively (Fig.4). In other words, a low level of monodispersity is indicative of less crystalline distortion and the above result verifies that ECO-T6 performs comparatively to crystalline distortion capability of the COMP. This result further supports the fact that two different inhibition mechanisms of $CaCO_3$ are made by the COMP and ECO-T6, which is confirmed based on SEM images and PSD analysis. Instead of inhibiting the formation of calcite made by the COMP, ECO-T6 containing a carboxylate group is likely to modify the stereochemical orientation of rhombohedric calcite[10], resulting in a structural failure and a reduction in surface energy of calcite for particle growth by flocculation.

3.2.3 XRD determination

Powder XRD analysis was carried out for the quantitative assessment for the composition of different polymorphs of $CaCO_3$ in each sample. Figure 5 depicts the XRD patterns of $CaCO_3$ obtained in the presence of ECO-T6 and COMP. The characteristic peaks at 29.4 and 26.3° in both cases of ECO-T6 and COMP confirmed the presence of calcite and vaterite while peaks corresponding to vaterite were absent in the control experiment. This phenomenon indicates that the involvement of antiscalant is thermodynamically favorable to the transformation of calcite into vaterite. This result is expected and consistent with the previous reports, as crystalline transformation of calcite is likely to take place in case where antiscalant is present[11,12]. In other words, vaterite grows at the expense of the calcite owing to the fact that antiscalant is able to disturb calcite growth.

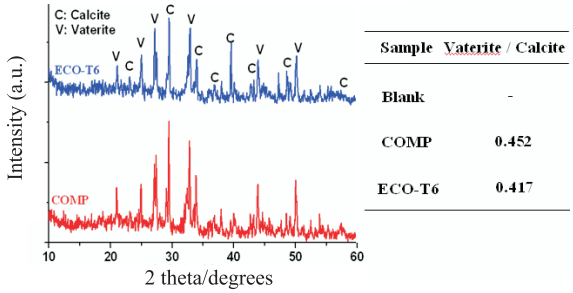

Fig.5. XRD patterns of $CaCO_3$ in the presence of antiscalants.

It was reported that the stability of scale significantly depends on the polymorphic composition of $CaCO_3$. For example, rhombohedric calcite forms a relatively strong adherence ability toward the pipe surface whereas the stereostructure of vaterite is unlikely to stack up. Calcite is also more stable when compared to vaterite in terms of the thermodynamic point of view. Therefore, the polymorph ratio of vaterite over calcite can be exploited for further evaluation in antiscalant performance. A higher vaterite/calcite ratio (V/C ratio) is an improved characteristic of an antiscalant's ability to distort calcite growth. As shown in Fig.5, the V/C ratio in the case of ECO-T6 is a little bit lower than that of the COMP, implying that the capability of ECO-T6 in selective transformation of calcite into vaterite is inferior to that of the COMP. The relatively excellent transformation capability of the COMP is also evident by the SEM images and PSD analysis, as vaterite polymorph exhibits spherical structure with a relatively small diameter.

3.3 $CaCO_3$ crystalline kinetics in the absence and presence of antiscalant

Studies relating to the measurement of formation kinetics of scales are rare despite several attempts having claimed some reliable approaches. For example, focused beam reflectance[13,14] and chronoamperometric measurements[15,16] are two common methods. An alternative method was also proposed in this study to examine the scaling kinetics in the static condition based on light scattering spectroscopy. Any destabilization phenomenon happening in a given time would have an effect on its values of backscattering or transmission intensities during aging. Based on this concept, an index by the name of Turbiscan Stability Index (TSI) was developed by The Formulaction Company to monitor the variation of light intensity detected in the

sample. A (TSI) index was obtained by comparing mathematically the light intensity based on a scan-to-scan difference and it sums all the variations detected in the sample. At a given ageing time, the higher value in the TSI, the worse stability of the sample. In other words, TSI as a function of time accounts for the formation kinetics of $CaCO_3$ scaling.

As shown in Fig.6, the curves in both cases of control experiment and the COMP are characterized by appearance of two regions. The former one likely features the growth stage of $CaCO_3$ whereas the later one indicates that the reaction reaches a plateau. This result is reasonable because the formation kinetics of $CaCO_3$ mitigates with decreasing concentration of calcium ions, which is corresponding to the concentration profile shown in Fig.1. In addition, an inspiring phenomenon was observed in the formation kinetics of $CaCO_3$ in the control experiment and the COMP sample are first-order reactions whereas $CaCO_3$ formation in the presence of ECO-T6 follows zero order kinetics. Since a zero-order reaction features an independent reaction without respect to the reactant concentration, the reaction rate speeds up only in the case of a catalyst being involved in the formation mechanism of $CaCO_3$. It was believed that the regular formation mechanism of $CaCO_3$ was altered with ECO-T61. To the best of our knowledge, as far, no report is available to examine the formation mechanism and kinetics of $CaCO_3$ based on the light scattering spectrometry. On the other hand, a quantified value of kinetics of $CaCO_3$ formation in the presence of ECO-T6 was 72.9 TSI h^{-1}, which is less than that of the COMP by almost six-fold. This result is consistent with the fact that the ion dispersion capacity offered by ECO-T6 is superior to that of the COMP, as shown in the concentration profile of calcium ion (Fig.1).

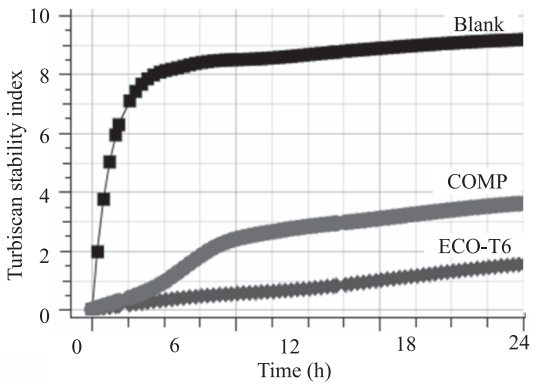

Fig.6. TSI values as a function of time in the absence and presence of antiscalants.

4. CONCLUSION

To break the tradeoff between environmental policy and economic growth, an environmental relief antiscalant with relatively low phosphate content, ECO-T6, was developed in this study. The anti-scale properties of ECO-T6 towards $CaCO_3$ in the artificial cooling water were studied through static scale inhibition tests. It was shown that ECO-T6 highlighted a comparative capability towards suppressing $CaCO_3$ formation, with an approximately 98.1% efficiency at a level of 4 mg/L phosphate, which is only half that of the COMP. SEM images, PSD analysis and XRD patterns identified a particular inhibition mechanism of $CaCO_3$ formation made by ECO-T6, which was comprehensively different from that of the COMP. This is because ECO-T6 is able to recognize and react with positively charged calcium ions to form a stabilized and dissoluble calcium-complex. The formation kinetics of $CaCO_3$ was also investigated base on light scattering spectrometry in that $CaCO_3$ formation kinetics in the presence of ECO-T6 is six times lower than that of the COMP. From an environmental point of view, broad field applications of our developed antiscalant for open-loop cooling water systems are expected in the near future.

REFERENCES

1. A. L. Kavitha, T. Vasudevan and H. Gurumallesh Prabu: Desalination, 2011, vol. 268, pp. 38-45.
2. L. N. Plummer and E. Busenberg: Geochim. Cosmochim. Acta: 1982, vol. 46, pp. 1011-1040.
3. Y. P. Lin and P. C. Singer: Water Research, 2005, vol. 39, pp. 4835-4843.
4. D. Heath, B. Sirok, M. Hocevar and B. Pecnik: Journal of Mechanical Engineering, 2013, vol. 59, pp. 203- 215.
5. M. Gryta: Desalination, 2012, vol. 285, pp. 170-176.
6. Y. Xu, L. Zhao, L. Wang, S. Xu and Y. Cui: Desalination, 2012, vol. 286, pp. 285-289.
7. B. E. Huntsman, C. A. Staples, C. G. Naylor and J. B. Williams: Water Environmental Research, 2006, vol. 78, pp. 2397-2404.
8. S. P. Gopi and V. K. Subramanian: Desalination, 2012, vol. 297, pp. 38-47.
9. L. F. Greenlee, F. Testa, D. F. Lawler, B. D. Freeman and P. Moulin: Water Research, 2010, vol. 44, pp. 2957-2969.
10. Z. Shen, J. Li, K. Xu, L. Ding and H. Ren: Desalination, 2012, vol. 284, pp. 238-244.
11. Y. M. Tang, W. Z. Yang, X. S. Yin, Y. Liu, P. W. Yin and J. T. Wang: Desalination, 2008, vol. 228, pp. 55-60.
12. Q. F. Yang, Y. Q. Liu, A. H. Gu, J. Ding and Z. Q. Shen: Journal of Colloid and Interface Science, 2001, vol. 240, pp. 608-621.

13. W. N. Al Nasser, A. Shaikh, C. Morriss, C. Hounslow, M. J. Hounslow and A. D. Salman: Chemical Engineering Science, 2008, vol. 65, pp. 1381-1389.
14. W. N. Al Nasser and F. H. Al Salhi: Chemical Engineering Science, 2013, vol. 86, pp. 70-77.
15. D. E. Abd-El-Khalek and B. A. Abd-Cl-Nabey: Desalination, 2013, vol. 311, pp. 227-233.
16. R. Ketrane, B. Saidani, O. Gil, L. Leleyter and F. Baraud: Desalination, 2009, vol. 249, pp. 1397-1404.
□